Multiscale modeling of calcium cycling in cardiac ventricular myocyte: Macroscopic consequences of microscopic dyadic function

Namit Gaur[†] and Yoram Rudy[†*]

Supplementary Information

† Department of Biomedical Engineering and Cardiac Bioelectricity and Arrhythmia Center, Washington University in Saint Louis

* Corresponding Author:

Yoram Rudy

Campus Box 1097

Washington University in St. Louis

St. Louis, MO 63130-4899

e-mail: rudy@wustl.edu

phone: (314) 935-8160

fax: (314) 935-8168

Keywords: Ca spark, Ca wave, dyad, luminal Ca sensor, multiscale model, stochastic Ca release process

Table of Contents

DEFINITIONS AND ABBREVIATIONS 3
Cell Geometry 3
Currents 3
Gates 4
Conductances and Permeability 4
Concentrations 4
Fluxes 5
Buffers 5
Rates and Time Constants 5
Reversal Potentials 5
Others 6
MODEL PARAMETERS 6
Cell Geometry 6
External Concentrations 7
Initial Conditions 7
Stimulus 7
MODEL CURRENTS 7
Fast Sodium Current 7
Fast Component of Delayed Rectifier K Current 8
Slow Component of Delayed Rectifier K Current 9
Inward Rectifier K Current 9
Sodium Potassium Pump Current 10
Background Sodium Current 10
Plateau K Current 10
L-type Ca Current 10
Background Ca Current 12
T-type Ca Current 12
Sarcolemmal Ca Pump Current 13
Na-Ca Exchange Current in the Myoplasm 13
Na-Ca Exchange Current in the Submembrane Space 13
Voltage 13

MODEL FLUXES **14**
SR Ca release 14
Ca Diffusion fluxes 15
Ca Uptake in the NSR 16
Ca Leak from NSR 16
MODEL CONCENTRATIONS AND BUFFERS **16**
Ca Concentration in the Dyadic Space 16
Ca Concentration in the Submembrane Space 17
Ca Concentration in the JSR 17
Ca Concentration in the NSR 17
Ca Concentration in the Myoplasm 17
Na Concentration in the Myoplasm 18
K Concentration in the Myoplasm 18
ADDITIONAL METHODS AND DISCUSSION **18**
Stochastic Model of Ca Cycling 18
Simulation Methods 18
SUPPLEMENTARY FIGURES **20**

DEFINITIONS AND ABBREVIATIONS

Cell Geometry

V_{cell}	Volume of the cell (μL)
A_{cap}	Capacitive membrane area (cm^2)
V_i	Volume of the myoplasm (μL)
V_{NSR}	Volume of the network sarcoplasmic reticulum (NSR) (μL)
V_{JSR}	Volume of the junctional sarcoplasmic reticulum (JSR) (μL)
V_{ss}	Volume of the submembrane space (μL)
N_{total_dyads}	Total number of dyads in the cell
v_i^n	Volume of the nth dyadic myoplasm (μL)
v_{ss}^n	Volume of the nth dyadic submembrane space (μL)
v_{NSR}^n	Volume of the nth dyadic NSR (μL)
v_{JSR}^n	Volume of the nth dyadic JSR (μL)
v_{ds}^n	Volume of the nth dyadic space volume (μL)
N_{LCC}^n	Number of L-type channels (LCCs) in the nth dyad
N_{RyR2}^n	Number of Ryanodine Receptors (RyR2s) in the nth dyad

Currents

I_{ion}	Total ionic current ($\mu A/\mu F$)
I_{Na}	Fast Na current ($\mu A/\mu F$)
I_{CaL}^{cell}	Whole-cell L-type Ca current ($\mu A/\mu F$)
I_{CaNa}	Na current through LCCs ($\mu A/\mu F$)
I_{CaK}	K current through LCCs ($\mu A/\mu F$)
I_{Cat}^{cell}	Whole-cell T-type Ca current ($\mu A/\mu F$)
I_{Kr}	Rapid delayed rectifier K current ($\mu A/\mu F$)
I_{Ks}	Slow delayed rectifier K current ($\mu A/\mu F$)
I_{K1}	Time independent K current ($\mu A/\mu F$)
I_{NaCa}^{cell}	Whole-cell myoplasmic Na-Ca exchanger current ($\mu A/\mu F$)
$I_{NaCa,ss}^{cell}$	Whole-cell submembrane Na-Ca exchanger current ($\mu A/\mu F$)
I_{NaK}	Na-K pump current ($\mu A/\mu F$)
I_{Nab}	Background Na current ($\mu A/\mu F$)
I_{pCa}^{cell}	Whole-cell current through sarcolemmal Ca pump ($\mu A/\mu F$)
I_{Cab}^{cell}	Whole-cell background Ca current ($\mu A/\mu F$)
I_{Kp}	Plateau K current ($\mu A/\mu F$)
$\overline{I_{Ca}}$	Maximum Ca current through LCCs ($\mu A/\mu F$)
I_{CaL}^n	L-type Ca current in the nth dyad ($\mu A/\mu F$)
I_{Cab}^n	Background Ca current in the nth dyad ($\mu A/\mu F$)
I_{Cat}^n	T-type Ca current in the nth dyad ($\mu A/\mu F$)
I_{pCa}^n	Sarcolemmal pump current in the nth dyad ($\mu A/\mu F$)
I_{NaCa}^n	Na-Ca exchanger current in the myoplasm in the nth dyad ($\mu A/\mu F$)
$I_{NaCa,ss}^n$	Na-Ca exchanger current in the submembrane space in the nth dyad ($\mu A/\mu F$)
$\bar{I}_{CaNa}$	Maximum Na current through LCCs ($\mu A/\mu F$)

$\bar{I}_{CaK}$	Maximum K current through LCCs $(\mu A/\mu F)$
I_{st}	Stimulus current $(\mu A/\mu F)$

Gates

m	Activation gate of Na current
h	Fast inactivation gate of Na current
j	Slow inactivation gate of Na current
x_r	Activation gate of I_{Kr}
r_{kr}	Time-independent rectification gate of I_{Kr}
x_{s1}	Fast activation gate of I_{Ks}
x_{s2}	Slow activation gate of I_{Ks}
K_1	Inactivation gate of I_{K1}
K_p	Fast activation gate of I_{Kp}
b	Activation gate of T-type Ca current
g	Inactivation gate of T-type Ca current

Conductances and Permeability

G_{Na}	Maximum conductance of I_{Na} $(mS/\mu F)$
G_{Nab}	Maximum conductance of I_{Nab} $(mS/\mu F)$
G_{Kr}	Maximum conductance of I_{Kr} $(mS/\mu F)$
$P_{Na,K}$	Permeability ratio of Na ion to K ion
G_{Ks}	Maximum conductance of I_{Ks} $(mS/\mu F)$
G_{K1}	Maximum conductance of I_{K1} $(mS/\mu F)$
G_{Kp}	Maximum conductance of I_{Kp} $(mS/\mu F)$
G_{NaK}	Maximum conductance of I_{NaK} $(mS/\mu F)$
P_{Ca}	Permeability of membrane to Ca (cm/s)
P_{Na}	Permeability of membrane to Na (cm/s)
P_K	Permeability of membrane to K (cm/s)

Concentrations

Na_o	Extracellular Na concentration (mM)
Na_i	Intracellular Na concentration (mM)
K_i	Intracellular K concentration (mM)
K_o	Extracellular K concentration (mM)
Ca_o	Extracellular Ca concentration (mM)
Ca_{JSR}^n	Free JSR Ca concentration in the nth dyad (mM)
Ca_{NSR}^n	Free NSR Ca concentration in the nth dyad (mM)
Ca_d^n	Dyadic space Ca concentration in the nth dyad (μM)
Ca_{ss}^n	Submembrane Ca concentration in the nth dyad (mM)
Ca_i^n	Myoplasmic Ca concentration in the nth dyad (mM)
Ca_i^{cell}	Whole-cell Ca concentration in the myoplasm (mM)
Ca_{ss}^{cell}	Whole-cell Ca concentration in the submembrane space (mM)
Ca_d^{cell}	Whole-cell Ca concentration in the dyadic space (μM)
Ca_{NSR}^{cell}	Whole-cell Ca concentration in the NSR (mM)
Ca_{JSR}^{cell}	Whole-cell Ca concentration in the JSR (mM)

$\overline{NSR}$	Maximum Ca concentration in the NSR (mM)

Fluxes

J^n_{CaL}	Ca flux through LCCs in the nth dyad $(\mu M/ms)$
J^n_{rel}	Ca release flux in the nth dyad $(\mu M/ms)$
J^n_{Cadiff}	Diffusive Ca flux into the nth dyadic space from adjacent dyadic spaces $(\mu M/ms)$
$J^n_{NSRdiff}$	Diffusive Ca flux into the nth dyadic NSR from adjacent dyadic NSRs (mM/ms)
$J^n_{Cadiff\_ds\_ss}$	Diffusive Ca flux from dyadic space into submembrane space $(\mu M/ms)$
$J^n_{Cadiff\_ss\_i}$	Diffusive Ca flux from submembrane space into the myoplasm $(\mu M/ms)$
$J^n_{Cadiff\_NSR\_JSR}$	Translocation Ca flux from NSR to JSR (mM/ms)
J^n_{up}	Uptake Ca flux into NSR from the myoplasm in the nth dyad $(\mu M/ms)$
$\overline{I_{up}}$	Maximum rate of Ca uptake into NSR $(\mu M/ms)$
J^n_{leak}	SR leak into NSR in the nth dyad (mM/ms)

Buffers

$csqn$	Free calsequestrin (CSQN) concentration (mM)
$csqn.ca$	Ca-bound CSQN concentration (mM)
K_{mcsqn}	Half-saturation constant of Ca binding of CSQN (mM)
$\overline{csqn}$	Total concentration of CSQN (mM)
B_{ss}	Instantaneous buffering factor in submembrane space
B_{JSR}	Instantaneous buffering factor in JSR
B_{myo}	Instantaneous buffering factor in myoplasm
$\overline{TRPN}$	Maximum concentration of Troponin C buffer (mM)
$\overline{CMDN}$	Maximum concentration of Calmodulin (mM)
K_{mTRPN}	Half-saturation constant of Ca binding of Troponin C (mM)
K_{mCMDN}	Half-saturation constant of Ca binding of Calmodulin (mM)

Rates and Time Constants

k_{xy}	Transition rate between state x and y in LCC or in RyR2 (ms^{-1})
τ_{efflux}	Time-constant of Ca diffusion from the dyadic space into the submembrane space (ms)
τ_{refill}	Time-constant of Ca translocation from NSR to JSR (ms)
$\tau_{diff\_ds\_ds}$	Time-constant of Ca diffusion between dyadic spaces (ms)
$\tau_{diff\_NSR\_NSR}$	Time-constant of Ca diffusion between dyadic NSRs (ms)
d_{ryr}	Diffusion rate of Ca through open RyR2 (ms^{-1})

Reversal Potentials

E_{Na}	Reversal potential of Na current (mV)
E_K	Reversal potential of I_{Kr} and I_{K1} current (mV)
E_{Ks}	Reversal potential of I_{Ks} (mV)
E^n_{Ca}	Reversal potential of Ca in the nth dyad (mV)

Others

C_m	Total cellular membrane capacitance ($\mu F/cm^2$)
V_m	Transmembrane potential (mV)
F	Faraday constant (C/mol)
R	Gas constant ($J/kmol/K$)
T	Temperature (K)
BCL	Basic Cycle Length (ms)
$K_{m,Nai}$	Half saturation constant of Na for I_{NaK}
$K_{m,Ko}$	Half saturation constant of K for I_{NaK}
K_{mpCa}	Half saturation concentration for sarcolemmal Ca pump (mM)
K_{mup}	Half-saturation constant of SR Ca uptake into NSR (mM)
σ	Na_o - dependent factor of f_{NaK}
f_{NaK}	Voltage-dependent factor of I_{NaK}
$\gamma_{Cai},\ \gamma_{Cao}$	Activity coefficient of Ca
γ_s	Position of energy barrier controlling voltage-dependence of Na-Ca exchanger current
$\gamma_{Nai},\ \gamma_{Nao}$	Activity coefficient of Na
$\gamma_{Ki},\ \gamma_{Ko}$	Activity coefficient of K
z_{Ca}	Valence state of Ca
z_{Na}	Valence state of Na
z_K	Valence state of K
$N^n_{open\ LCC}$	Number of open LCCs in a dyad
$N^n_{open\ RyR2}$	Number of open RyR2s in the nth dyad
LCC	L-type channel
RyR2	Type 2 isoform of Ryanodine Receptor

MODEL PARAMETERS

Cell Geometry

$V_{cell} = 38 \cdot 10^{-6}\ \mu L$
$A_{cap} = 1.534 \cdot 10^{-4}\ cm^2$
$V_i = 25.84 \cdot 10^{-6}\ \mu L$
$V_{NSR} = 2.098 \cdot 10^{-6}\ \mu L$
$V_{JSR} = 0.182 \cdot 10^{-6}\ \mu L$
$V_{ss} = 0.76 \cdot 10^{-6}\ \mu L$
$N_{total\_dyads} = 10{,}000$

It is assumed that the submembrane space occupies a depth of 50 nm from the surface membrane. If an individual dyadic space occupies an area of 130 nm X 130 nm and if we assume that there are 10,000 dyads in a ventricular myocyte, V_{ss} can be derived as: $V_{ss} = (A_{cap} - N_{total\_dyads} \cdot A_{ds}) \cdot 50\ nm = 0.76 \cdot 10^{-6}\ \mu L$, where A_{ds} is the area occupied by an individual dyadic space. This space is equal to 2% of V_{cell}. All other values are taken from (1).

$$v_i^n = \frac{V_i}{N_{total\_dyads}}$$

$v_{ss}^n = \frac{V_{ss}}{N_{total\_dyads}}$
$v_{NSR}^n = \frac{V_{NSR}}{N_{total\_dyads}}$
$v_{JSR}^n = \frac{V_{JSR}}{N_{total\_dyads}}$
$v_{ds}^n = 2 \cdot 10^{-13}\ \mu L$
$N_{LCC}^n = 15$
$N_{RyR2}^n = 100$

The volume of dyadic space is assumed to occupy the dimensions 130 nm X 130 nm in area and 12 nm in height representing the distance between LCCs and RyR2s.

External Concentrations

$Na_o = 140\ mM$
$Ca_o = 2\ mM$
$K_o = 4.5\ mM$

Initial Conditions

$V_m = -86.364\ mV$
$m = 0.001231$
$h = 0.988864$
$j = 0.992842$
$xs_1 = 0.00611$
$xs_2 = 0.029537$
$xr = 0.000175$
$b = 0.001229$
$g = 0.991057$
$Na_i = 12.6233\ mM$
$K_i = 124.383\ mM$
$Ca_i^n = 8.83 \cdot 10^{-5}\ mM$
$Ca_{ss}^n = 8.04 \cdot 10^{-5}\ mM$
$Ca_d^n = 8.04 \cdot 10^{-2}\ \mu M$
$Ca_{JSR}^n = 1.29871\ mM$
$Ca_{NSR}^n = 1.29892\ mM$

Monte Carlo simulations determine the initial state of each LCC and RyR2 based on transition rates determined by the initial conditions.

Stimulus

A stimulus current (I_{st}) of -80 μA/μF amplitude for a duration of 0.5 ms is used to pace the cell. The current is assumed to be K current (2).

MODEL CURRENTS

Fast Sodium Current

$G_{Na} = 16$

$$F = 96500$$
$$R = 8310$$
$$T = 310$$
$$E_{Na} = \left(\frac{R \cdot T}{F}\right) \cdot ln\left(\frac{Na_o}{Na_i}\right)$$
$$\alpha_m = \frac{\left(0.32 \cdot (V_m + 47.13)\right)}{\left(1 - exp\left(-0.1 \cdot (V_m + 47.13)\right)\right)}$$
$$\beta_m = 0.08 \cdot exp\left(\frac{-V_m}{11}\right)$$
If (V_m < -40)
$$\alpha_j = \frac{\left(\left(-127140 \cdot exp(0.2444 \cdot V_m) - 3.474 \cdot 10^{-5} \cdot exp(-0.04391 \cdot V_m)\right)(V_m + 37.78)\right)}{\left(1 + exp\left(0.311 \cdot (V_m + 79.23)\right)\right)}$$
$$\beta_j = \frac{(0.1212 \cdot exp(-0.01052 \cdot V_m))}{\left(1 + exp\left(-0.1378 \cdot (V_m + 40.14)\right)\right)}$$
$$\alpha_h = 0.135 \cdot exp\left(\frac{80 + V_m}{-6.8}\right)$$
$$\beta_h = 3.56 \cdot exp(0.079 \cdot V_m) + 3.1 \cdot 10^5 \cdot exp(0.35 \cdot V_m)$$
If (V_m ≥-40)
$$\alpha_h = \alpha_j = 0$$
$$\beta_h = \frac{1}{\left(0.13 \cdot \left(1 + exp\left(\frac{(V_m + 10.66)}{-11.1}\right)\right)\right)}$$
$$\beta_j = \frac{0.3 \cdot exp(-0.0000002535 \cdot V_m)}{1 + exp\left(-0.1 \cdot (V_m + 32)\right)}$$
$$\frac{dm}{dt} = \alpha_m \cdot m - \beta_m \cdot (1 - m)$$
$$\frac{dh}{dt} = \alpha_h \cdot h - \beta_h \cdot (1 - h)$$
$$\frac{dj}{dt} = \alpha_j \cdot j - \beta_j \cdot (1 - j)$$
$$I_{Na} = G_{Na} \cdot m^3 \cdot h \cdot j \cdot (V_m - E_{Na})$$

Fast Component of Delayed Rectifier K Current

$$G_{Kr} = 0.02614 \cdot \sqrt{\frac{K_o}{5.4}}$$
$$E_K = \left(\frac{R \cdot T}{F}\right) \cdot ln\left(\frac{K_o}{K_i}\right)$$
$$x_{rss} = \frac{1}{\left(1 + exp\left(-\frac{(V_m + 21.5)}{7.5}\right)\right)}$$

$$\tau_{xr} = \frac{1}{\frac{1.38 \cdot 10^{-3} \cdot (V_m + 14.2)}{1 - exp\left(-0.123 \cdot (V_m + 14.2)\right)} + \frac{6.1 \cdot 10^{-4} \cdot (V_m + 38.9)}{exp\left(0.145 \cdot (V_m + 38.9)\right) - 1}}$$

$$r_{kr} = \frac{1}{1 + exp\left(\frac{V_m + 9}{18.4}\right)}$$

$$\frac{dx_r}{dt} = \frac{x_{rss} - x_r}{\tau_{xr}}$$

$$I_{kr} = G_{kr} \cdot x_r \cdot r_{kr} \cdot (V_m - E_K)$$

Slow Component of Delayed Rectifier K Current

$$P_{Na,K} = 0.01833$$

$$G_{Ks} = 0.3031 \cdot \left(1 + \frac{0.6}{1 + \left(\frac{3.8 \cdot 10^{-5}}{Ca_i^{cell}}\right)^{1.4}}\right)$$

$$E_{Ks} = \left(\frac{R \cdot T}{F}\right) \cdot ln\left(\frac{K_o + P_{Na,K} \cdot Na_o}{K_i + P_{Na,K} \cdot Na_i}\right)$$

$$x_{s1ss} = x_{s2ss} = \frac{1}{1 + exp\left(\frac{1.5 - V_m}{16.7}\right)}$$

$$\tau_{xs1} = \frac{1}{\frac{7.19 \cdot 10^{-5} \cdot (V_m + 30)}{1 - exp\left(-0.148 \cdot (V_m + 30)\right)} + \frac{1.31 \cdot 10^{-4} \cdot (V_m + 30)}{exp\left(0.0687 \cdot (V_m + 30)\right) - 1}}$$

$$\tau_{xs2} = 4 \cdot \tau_{xs1}$$

$$\frac{dx_{s1}}{dt} = \frac{x_{s1ss} - x_{s1}}{\tau_{xs1}}$$

$$\frac{d_{xs2}}{dt} = \frac{x_{s2ss} - x_{s2}}{\tau_{xs2}}$$

$$I_{ks} = G_{ks} \cdot x_{s1} \cdot x_{s2} \cdot (V_m - E_{Ks})$$

Inward Rectifier K Current

$$G_{K1} = 0.75 \cdot \sqrt{\frac{K_o}{5.4}}$$

$$E_K = \left(\frac{R \cdot T}{F}\right) \cdot ln\left(\frac{K_o}{K_i}\right)$$

$$\alpha_{K1} = \frac{1.02}{1 + exp\left(0.2385 \cdot (V_m - E_K - 59.215)\right)}$$

$$\beta_{K1} = \frac{0.49124 \cdot exp\left(0.08032 \cdot (V_m - E_K + 5.476)\right) + exp\left(0.06175 \cdot (V_m - E_K - 594.31)\right)}{1 + exp\left(-0.5143 \cdot (V_m - E_K + 4.753)\right)}$$

$$K_1 = \frac{\alpha_{K1}}{\alpha_{K1} + \beta_{K1}}$$

$$I_{K1} = G_{K1} \cdot K_1 \cdot (V_m - E_K)$$

Sodium Potassium Pump Current

$$G_{NaK} = 2.25$$

$$\sigma = \frac{exp\left(\frac{Na_o}{67.3}\right) - 1}{7}$$

$$f_{NaK} = \frac{1}{1 + 0.1245 \cdot exp\left(\frac{-0.1 \cdot V_m \cdot F}{R \cdot T}\right) + 0.0365 \cdot \sigma \cdot exp\left(\frac{-V_m \cdot F}{R \cdot T}\right)}$$

$$K_{m,Nai} = 10$$

$$K_{m,Ko} = 1.5$$

$$I_{NaK} = G_{NaK} \cdot \frac{f_{NaK}}{1 + \left(\frac{K_{m,Nai}}{Na_i}\right)^2} \cdot \left(\frac{K_o}{K_o + K_{m,Ko}}\right)$$

Background Sodium Current

$$G_{Nab} = 0.004$$

$$E_{Na} = \left(\frac{R \cdot T}{F}\right) \cdot ln\left(\frac{Na_o}{Na_i}\right)$$

$$I_{Nab} = G_{Nab} \cdot (V_m - E_{Na})$$

Plateau K Current

$$G_{Kp} = 5.52 \cdot 10^{-3}$$

$$E_K = \left(\frac{R \cdot T}{F}\right) \cdot ln\left(\frac{K_o}{K_i}\right)$$

$$K_p = \frac{1}{1 + exp\left(\frac{7.488 - V_m}{5.98}\right)}$$

$$I_{Kp} = G_{Kp} \cdot K_p \cdot (V_m - E_K)$$

L-type Ca Current

The LCC scheme is same as in (1). Kinetic state of every single LCC in the model is monitored. Monte-Carlo simulations determine the state of LCC in the next time step based on transition rates shown below.

Transition Rates Between States

$$\alpha = 0.925 \cdot exp\left(\frac{V_m}{30}\right)$$

$$\beta = 0.39 \cdot exp\left(\frac{-V_m}{40}\right)$$

$$k_{C1C2} = 4 \cdot \alpha$$

$$k_{C2C3} = 3 \cdot \alpha$$

$$k_{C3C4} = 2 \cdot \alpha$$

$$k_{C4O} = \alpha$$

$$k_{OC4} = 4 \cdot \beta$$

$$k_{C4C3} = 3 \cdot \beta$$

$$k_{C3C2} = 2 \cdot \beta$$
$$k_{C2C1} = \beta$$
$$k_{C3IVs} = 0.005 \cdot exp\left(\frac{-V_m}{40}\right)$$
$$k_{C3IVf} = 0.245 \cdot exp\left(\frac{V_m}{10}\right)$$
$$k_{OIVs} = 0.03 \cdot exp\left(\frac{-V_m}{280}\right)$$
$$k_{OIVf} = 0.02 \cdot exp\left(\frac{V_m}{500}\right)$$
$$k_{IVsO} = 0.0011 \cdot exp\left(\frac{V_m}{500}\right)$$
$$k_{IVfO} = 0.035 \cdot exp\left(\frac{-V_m}{300}\right)$$
$$k_{IVsIVf} = \frac{k_{IVsO} \cdot k_{OIVf}}{k_{IVfO}}$$
$$k_{IVfIVs} = k_{OIVs}$$
$$k_{IVsC3} = \frac{k_{OC3} \cdot k_{IVsO} \cdot k_{C3IVs}}{k_{C3O} \cdot k_{OIVs}}$$
$$k_{IVfC3} = \frac{k_{OC3} \cdot k_{IVfO} \cdot k_{C3IVf}}{k_{C3O} \cdot k_{OIVf}}$$

Ca-dependent Inactivation Transition Rates

$$k_{Mode\ V-Mode\ Ca} = \frac{1}{1 + \frac{1}{Ca_d^n \cdot 10^{-3}}}$$
$$k_{Mode\ Ca-Mode\ V} = 0.01$$

LCC is open when the channel is in state O and in Mode V.

$$\bar{I}_{Ca} = P_{Ca} \cdot z_{Ca}^2 \cdot \frac{V_m \cdot F^2}{R \cdot T} \cdot \frac{\gamma_{Cai} \cdot Ca_d^n \cdot 10^{-3} \cdot exp\left(\frac{z_{Ca} \cdot V_m \cdot F}{R \cdot T}\right) - \gamma_{Cao} \cdot Ca_o}{exp\left(\frac{z_{Ca} \cdot V_m \cdot F}{R \cdot T}\right) - 1}$$
$$P_{Ca} = 6.075 \cdot 10^{-4}$$
$$\gamma_{Cai} = 0.01$$
$$\gamma_{Cao} = 0.341$$
$$z_{Ca} = 2$$
$$I_{CaL}^n = \bar{I}_{Ca} \cdot \left(\frac{N_{open\ LCC}^n}{N_{LCC}^n}\right)$$
$$I_{CaL}^{cell} = \frac{\sum_{n=1}^{n=N_{total\_dyads}} I_{CaL}^n}{N_{total\_dyads}}$$
$$J_{CaL}^n = \frac{-I_{CaL}^n}{2 \cdot v_{ds}^n \cdot F} \cdot \left(\frac{A_{cap}}{N_{total\_dyads}}\right) \cdot 1000$$

The transition rate into Ca-dependent inactivation tier, $k_{Mode\,V-Mode\,Ca}$ and P_{Ca} were modified to reproduce I_{CaL}^{cell} during pacing in a guinea pig ventricular myocyte.

Sodium (Na) Current through L-type Channels

$$\bar{I}_{CaNa} = P_{Na} \cdot z_{Na}^2 \cdot \frac{V_m \cdot F^2}{R \cdot T} \cdot \frac{\gamma_{Nai} \cdot Na_i \cdot exp\left(\frac{z_{Na} \cdot V_m \cdot F}{R \cdot T}\right) - \gamma_{Nao} \cdot Na_o}{exp\left(\frac{z_{Na} \cdot V_m \cdot F}{R \cdot T}\right) - 1}$$

$P_{Na} = 1.518 \cdot 10^{-6}$
$\gamma_{Nai} = 0.75$
$\gamma_{Nao} = 0.75$
$z_{Na} = 1$

$$I_{CaNa} = \bar{I}_{CaNa} \cdot \sum_{n=1}^{n=N_{total\_dyads}} \frac{N_{open\,LCC}^n}{N_{LCC}^n}$$

Potassium (K) Current through L-type Channels

$$\bar{I}_{CaK} = P_K \cdot z_K^2 \cdot \frac{V_m \cdot F^2}{R \cdot T} \cdot \frac{\gamma_{Ki} \cdot K_i \cdot exp\left(\frac{z_K \cdot V_m \cdot F}{R \cdot T}\right) - \gamma_{Ko} \cdot K_o}{exp\left(\frac{z_K \cdot V_m \cdot F}{R \cdot T}\right) - 1}$$

$P_K = 4.34 \cdot 10^{-7}$
$\gamma_{Ki} = 0.75$
$\gamma_{Ko} = 0.75$
$z_K = 1$

$$I_{CaK} = \bar{I}_{CaK} \cdot \sum_{n=1}^{n=N_{total\_dyads}} \frac{N_{open\,LCC}^n}{N_{LCC}^n}$$

Background Ca Current

$$E_{Ca}^n = \left(\frac{R \cdot T}{2 \cdot F}\right) \cdot ln\left(\frac{Ca_o}{Ca_i^n}\right)$$
$$I_{Cab}^n = 0.003016 \cdot (V_m - E_{Ca})$$
$$I_{Cab}^{cell} = \frac{\sum_{n=1}^{n=N_{total\_dyads}} I_{Cab}^n}{N_{total\_dyads}}$$

T-type Ca Current

$$b_{ss} = \frac{1}{1 + exp\left(\frac{-(V_m + 14)}{10.8}\right)}$$
$$\tau_b = 3.7 + \frac{6.1}{1 + exp\left(\frac{V_m + 25}{4.5}\right)}$$
$$g_{ss} = \frac{1}{1 + exp\left(\frac{V_m + 60}{5.6}\right)}$$

$$\tau_g = -0.875 \cdot V_m + 12 \ (V_m < 0);\ \tau_g = 12 \ (V_m \geq 0)$$
$$\frac{db}{dt} = \frac{b_{ss} - b}{\tau_b}$$
$$\frac{dg}{dt} = \frac{g_{ss} - g}{\tau_g}$$
$$I_{Cat}^n = 0.05 \cdot b \cdot b \cdot g \cdot (V_m - E_{Ca}^n)$$
$$I_{Cat}^{cell} = \frac{\sum_{n=1}^{n=N_{total\_dyads}} I_{Cat}^n}{N_{total\_dyads}}$$

Sarcolemmal Ca Pump Current

$$I_{pCa}^n = \frac{1.15 \cdot Ca_i^n}{Ca_i^n + K_{mpCa}}$$
$$K_{mpCa} = 0.0005$$
$$I_{pCa}^{cell} = \frac{\sum_{n=1}^{n=N_{total\_dyads}} I_{pCa}^n}{N_{total\_dyads}}$$

Na-Ca Exchange Current in the Myoplasm

$$c_1 = 0.00025$$
$$c_2 = 0.0001$$
$$c_3 = 1$$
$$\gamma = 0.15$$
$$z_{Ca} = 2$$
$$I_{NaCa}^n = \frac{c_1 \cdot exp\left(\frac{(\gamma - 1) \cdot V_m \cdot F}{R \cdot T}\right) \cdot \left(exp\left(\frac{V_m \cdot F}{R \cdot T}\right) \cdot Na_i^3 \cdot Ca_o - c_3 \cdot Na_o^3 \cdot Ca_i^n\right)}{1 + c_2 \cdot exp\left(\frac{(\gamma - 1) \cdot V_m \cdot F}{R \cdot T}\right) \cdot \left(exp\left(\frac{V_m \cdot F}{R \cdot T}\right) \cdot Na_i^3 \cdot Ca_o + c_3 \cdot Na_o^3 \cdot Ca_i^n\right)}$$
$$I_{NaCa}^{cell} = \frac{\sum_{n=1}^{n=N_{total\_dyads}} I_{NaCa}^n}{N_{total\_dyads}}$$

Na-Ca Exchange Current in the Submembrane Space

$$I_{NaCa,ss}^n = \frac{0.25 \cdot c_1 \cdot exp\left(\frac{(\gamma - 1) \cdot V_m \cdot F}{R \cdot T}\right) \cdot \left(exp\left(\frac{V_m \cdot F}{R \cdot T}\right) \cdot Na_i^3 \cdot Ca_o - c_3 \cdot Na_o^3 \cdot Ca_{ss}^n\right)}{1 + c_2 \cdot exp\left(\frac{(\gamma - 1) \cdot V_m \cdot F}{R \cdot T}\right) \cdot \left(exp\left(\frac{V_m \cdot F}{R \cdot T}\right) \cdot Na_i^3 \cdot Ca_o + c_3 \cdot Na_o^3 \cdot Ca_{ss}^n\right)}$$
$$I_{NaCa,ss}^{cell} = \frac{\sum_{n=1}^{n=N_{total\_dyads}} I_{NaCa,ss}^n}{N_{total\_dyads}}$$

Voltage

$$C_m = 1$$
$$I_{ion} = I_{Na} + I_{CaL}^{cell} + I_{CaNa} + I_{CaK} + I_{Cat}^{cell} + I_{Kr} + I_{Ks} + I_{K1} + I_{NaCa}^{cell} + I_{NaCa,ss}^{cell} + I_{NaK} + I_{Nab} + I_{pCa}^{cell} + I_{Cab}^{cell} + I_{Kp} + I_{st}$$
$$\frac{dV_m}{dt} = \frac{-I_{ion}}{C_m}$$

MODEL FLUXES

SR Ca release

Luminal Ca Sensor

CSQN can act both as SR Ca buffer (CSQN buffer) (3) and as a regulator of RyR2 openings (CSQN regulator) (4). The model of CSQN function can be interpreted biophysically as follows. Both free and Ca-bound CSQN form a relatively immobile network of protomers near RyR2s (CSQN network in Fig. S1), consistent with the scheme presented in (5). Diffusion of SR free Ca can occur readily in this network, thereby ensuring that the relative concentration of Ca-bound and free CSQN is spatially uniform in this network. Each RyR2 senses a proximal portion of the CSQN network in its vicinity (CSQN regulator in Fig. S1). In the RyR2 model (Fig. 1 *A* of main text), transition rate from the activation to the refractory tier is proportional to the concentration of free CSQN in the CSQN regulator domain, and the transition from the refractory to the activation tier is proportional to Ca-bound CSQN in this domain. In the CSQN network, the majority of CSQN acts as CSQN buffer (Fig. S1). This functional modeling scheme of luminal RyR2 regulation is based on the schemes depicted in (6) and (7). In the scheme presented in (6), the bulk of CSQN acts as SR Ca buffer. Single CSQN monomer binds to the Triadin/Junctin/RyR2 complex and modulates cytosolic Ca activation of RyR2. In the scheme presented in (7) CSQN binds to the Triadin/Junctin/RyR2 complex, making the channel refractory, and Ca-bound CSQN relieves this inhibition. The model was validated by comparing simulated open probability (P_o) of RyR2 at various SR and cytosolic Ca levels to single channel records measured in lipid bilayers (Fig. 2). The cell model was then fine-tuned to insure robust termination and appropriate restitution of SR Ca release in the whole cell, and accurate global Ca transients at all rates.

RyR2 Model

The RyR2 model scheme is shown in Fig. 1 *A*. The kinetic state of every single RyR2 in the model is monitored. Monte-Carlo simulations determine the state of each individual RyR2 in the next time step based on transition rates provided below. The activation and deactivation rates (k_{C1O1}, k_{O1C1}) and RyR2 channel conductance (d_{ryr}) were adapted from (8). The activation rate reflects the fact that Ca binds instantaneously to each of the subunits of the RyR2 tetramer before a slower Ca-independent transition to the open state occurs. The deactivation rate implies that the mean open time of the RyR2 channel is ~ 2 ms ($1/k_{O1C1}$). Considerations for inclusion of activation and refractory tiers in the RyR2 model are discussed in the "Luminal Ca Sensor" section of this Supplement. The transition rates between RyR2 tiers were constrained to reproduce accurately the local and global Ca concentrations and Ca currents in a guinea-pig myocyte during pacing at all rates.

Transition Rates

$$k_{C1O1} = \frac{3 \cdot (Ca_d^n)^4}{(Ca_d^n)^4 + (15)^4}$$

$$k_{O1C1} = 0.48$$

$$k_{C2O2} = \frac{3 \cdot (Ca_d^n)^4}{(Ca_d^n)^4 + (150)^4}$$

$$k_{O2C2} = 0.48$$

$$k_{C1C2} = 0.1 \cdot \left(\frac{csqn}{\overline{csqn}}\right)$$

$$k_{C2C1} = 0.1 \cdot \left(\frac{csqn.ca}{\overline{csqn}}\right) \cdot \frac{1}{1 + exp(0.9 \cdot BCL + t_{rel} - t)}$$
$$k_{O2O1} = k_{C2C1}$$
$$k_{O1O2} = k_{C1C2}$$

The dyad is considered active when the open fraction of RyR2s in the dyad is more than 0.2. t_{rel} is the time of last Ca release in the dyad, determined as the time at which open fraction of RyR2s in the dyad exceeds 0.2 upon activation of Ca release from the dyad.

$$J_{rel}^{n} = d_{ryr} \cdot N_{open\ RyR2}^{n} \cdot \left(1000 \cdot Ca_{JSR}^{n} - Ca_{d}^{n}\right)$$
$$d_{ryr} = 4$$
$$csqn = \frac{\overline{csqn} \cdot K_{mcsqn}}{\left(Ca_{jsr}^{n} + K_{mcsqn}\right)}$$
$$csqn.ca = \overline{csqn} - csqn$$
$$\overline{csqn} = 10$$
$$K_{mcsqn} = 0.8$$

Ca Diffusion fluxes

Inter-dyad coupling:

In ventricular myocytes, Ca diffusion can occur in both the cytosol and the SR (9). Under conditions of Ca overload, Ca released in a dyad can diffuse and trigger Ca release in adjacent dyads, forming traveling Ca waves (10); this provides evidence of cytosolic inter-dyad coupling. Model inter-dyad coupling in the cytosol was implemented by Ca diffusion between adjacent dyadic spaces. The parameters of diffusion were chosen so that Ca waves occur only under conditions of high SR load (with all other model parameters at control values). Simulated Ca release activity in a quiescent myocyte is shown in Fig. S4. With this choice of parameters, spontaneous Ca release activity in the form of Ca sparks, but not Ca waves, occurs when the initial SR load is low at 0.2 mM. Ca waves occur when the initial SR load is high at 5 mM.

Recent evidence suggests rapid diffusion of Ca in SR (9). Therefore, inter-dyad coupling in SR is implemented by fast Ca diffusion (time constant, $\tau_{diff\_NSR\_NSR}$ = 1 ms) between dyadic NSRs.

For $n > 1$ and $n < N_{total\_dyads}$

$$J_{Cadiff}^{n} = \frac{Ca_{d}^{n+1} - 2Ca_{d}^{n} + Ca_{d}^{n-1}}{\tau_{diff\_ds\_ds}}$$
$$\tau_{diff\_ds\_ds} = 15$$
$$J_{NSRdiff}^{n} = \frac{Ca_{NSR}^{n+1} - 2Ca_{NSR}^{n} + Ca_{NSR}^{n-1}}{\tau_{diff\_NSR\_NSR}}$$
$$\tau_{diff\_NSR\_NSR} = 1$$

For $n = 1$

$$J_{Cadiff}^{1} = \frac{Ca_{d}^{2} - Ca_{d}^{1}}{\tau_{diff\_ds\_ds}}$$
$$J_{NSRdiff}^{1} = \frac{Ca_{NSR}^{2} - Ca_{NSR}^{1}}{\tau_{diff\_NSR\_NSR}}$$

For $n = N_{total\_dyads}$

$$J_{Cadiff}^{N_{total\_dyads}} = \frac{Ca_d^{N_{total\_dyads}} - Ca_d^{N_{total\_dyads}-1}}{\tau_{diff\_ds\_ds}}$$

$$J_{NSRdiff}^{N_{total\_dyads}} = \frac{Ca_{NSR}^{N_{total\_dyads}} - Ca_{NSR}^{N_{total\_dyads}-1}}{\tau_{diff\_NSR\_NSR}}$$

Ca Diffusion from Dyadic Space into Submembrane Space

$$J_{Cadiff\_ds\_ss}^n = \frac{Ca_{ds}^n - Ca_{ss}^n}{\tau_{efflux}}$$

$\tau_{efflux} = 7 \cdot 10^{-4}$

τ_{efflux} is same as in (8).

Ca Diffusion from the Submembrane Space into the Myoplasm

$$J_{Cadiff\_ss\_i}^n = \frac{Ca_{ss}^n - Ca_i^n}{\tau_{diff\_ss\_i}}$$

$\tau_{diff\_ss\_i} = 0.1$

Ca Translocation from NSR to JSR

$$J_{Cadiff\_NSR\_JSR}^n = \frac{Ca_{NSR}^n - Ca_{JSR}^n}{\tau_{refill}}$$

$\tau_{refill} = 10$

τ_{refill} is same as in (8).

Ca Uptake in the NSR

$$J_{up}^n = \frac{\overline{I_{up}} \cdot Ca_i^n}{Ca_i^n + K_{mup}}$$

$\overline{I_{up}} = 0.00875;\ K_{mup} = 0.00092$

Ca Leak from NSR

$$J_{leak}^n = \frac{\overline{I_{up}} \cdot Ca_{NSR}^n}{\overline{NSR}}$$

$\overline{NSR} = 15$

MODEL CONCENTRATIONS AND BUFFERS

Ca Concentration in the Dyadic Space

$$Ca_d^n = J_{Cadiff}^n + \left(J_{rel}^n + J_{CaL}^n + \frac{Ca_{ss}^n}{\tau_{efflux}}\right) \cdot \tau_{efflux};\ \tau_{efflux} = 7.10^{-4}$$

$$Ca_d^{cell} = \frac{\sum_{n=1}^{n=N_{total\_dyads}} Ca_{ds}^n}{N_{total\_dyads}}$$

Note that we use the quasi-equilibrium approximation of Ca_d^n (11) since the time-scale over which Ca_d^n equilibrates with Ca_{ss}^n is much faster than other processes such as channel gating and Ca diffusion from adjacent dyads.

Ca Concentration in the Submembrane Space

$$B_{ss} = \frac{1}{1 + \frac{\overline{B_{SR}} \cdot K_{mSR}}{(Ca_{ss}^n + K_{mSR})^2} + \frac{\overline{B_{SL}} \cdot K_{mSL}}{(Ca_{ss}^n + K_{mSL})^2}}$$

$\overline{BSR} = 0.047$

$\overline{BSL} = 1.124$

$K_{mSR} = 0.00087$

$K_{mSL} = 0.0087$

$$\frac{dCa_{ss}^n}{dt} = -B_{ss} \cdot \left(-2I_{NaCa,ss}^n \cdot \left(\frac{A_{cap}}{N_{total\_dyads} \cdot z_{Ca} \cdot F \cdot v_{ss}^n} \right) + J_{Cadiff\_ss\_i}^n - 10^{-3} \cdot J_{Cadiff\_ds\_ss}^n \cdot \left(\frac{v_{ds}^n}{v_{ss}^n} \right) \right)$$

$$Ca_{ss}^{cell} = \frac{\sum_{n=1}^{n=N_{total\_dyads}} Ca_{ss}^n}{N_{total\_dyads}}$$

Ca Concentration in the JSR

$$B_{JSR} = \frac{1}{1 + \frac{\overline{csqn} \cdot K_{mcsqn}}{\left(Ca_{JSR}^n + K_{mcsqn}\right)^2}}$$

$$\frac{dCa_{JSR}^n}{dt} = B_{JSR} \cdot \left(-10^{-3} \cdot J_{rel}^n \cdot \left(\frac{v_{ds}^n}{v_{JSR}^n} \right) + J_{Cadiff\_NSR\_JSR}^n \right)$$

$$Ca_{JSR}^{cell} = \frac{\sum_{n=1}^{n=N_{total\_dyads}} Ca_{JSR}^n}{N_{total\_dyads}}$$

Ca Concentration in the NSR

$$\frac{dCa_{NSR}^n}{dt} = J_{NSRdiff}^n + \left(J_{up}^n - J_{leak}^n - J_{Cadiff\_NSR\_JSR}^n \cdot \left(\frac{v_{JSR}^n}{v_{NSR}^n} \right) \right)$$

$$Ca_{NSR}^{cell} = \frac{\sum_{n=1}^{n=N_{total\_dyads}} Ca_{NSR}^n}{N_{total\_dyads}}$$

Ca Concentration in the Myoplasm

$$B_{myo} = \frac{1}{1 + \frac{\overline{TRPN} \cdot K_{mTRPN}}{(Ca_i^n + K_{mTRPN})^2} + \frac{\overline{CMDN} \cdot K_{mCMDN}}{(Ca_i^n + K_{mCMDN})^2}}$$

$\overline{TRPN} = 0.07$

$K_{mTRPN} = 0.0005$

$$\overline{CMDN} = 0.05$$
$$K_{mCMDN} = 0.00238$$
$$\frac{dCa_i^n}{dt} = -B_{myo} \cdot \left(\left(I_{Cab}^n + I_{Cat}^n + I_{pCa}^n - 2 \cdot I_{NaCa}^n\right) \cdot \left(\frac{A_{cap}}{N_{total\_dyads} \cdot z_{Ca} \cdot F \cdot v_i^n}\right) + \left(J_{up}^n - J_{leak}^n\right) \cdot \left(\frac{v_{NSR}^n}{v_{cyt}^n}\right) - J_{Cadiff\_ss\_i}^n \cdot \left(\frac{v_{ss}^n}{v_{cyt}^n}\right) \right)$$
$$Ca_i^{cell} = \frac{\sum_{n=1}^{n=N_{total\_dyads}} Ca_i^n}{N_{total\_dyads}}$$

Na Concentration in the Myoplasm

$$\frac{dNa_i}{dt} = -\left(I_{Na} + I_{Nab} + I_{CaNa} + 3 \cdot I_{NaK} + 3 \cdot I_{NaCa}^{cell} + 3 \cdot I_{NaCa,ss}^{cell}\right) \cdot \left(\frac{A_{cap}}{F \cdot V_i \cdot z_{Na}}\right)$$

K Concentration in the Myoplasm

$$\frac{dK_i}{dt} = -\left(I_{Kr} + I_{Ks} + I_{K1} + I_{Kp} + I_{CaK} - 2 \cdot I_{NaK} + I_{st}\right) \cdot \left(\frac{A_{cap}}{F \cdot V_i \cdot z_K}\right)$$

ADDITIONAL METHODS AND DISCUSSION

Stochastic Model of Ca Cycling

Many existing models of Ca cycling in cardiac ventricular myocytes are deterministic, based on average, subcellular compartments representation (1, 12-13). They are not stochastic and are not formulated at the microscopic scale of local dyadic interaction between LCCs and RyR2s. Several models were developed to investigate local stochastic Ca release at the level of the dyadic space (14-16). There have been fewer attempts to link these processes to the whole myocyte behavior. One of these models (17) and its numerical simplification (18) described local control of Ca release during ECC. Other models (19-20) were used to study cardiac alternans. The task has proven arduous due to the large number of parameters involved and the large ratio of computing to simulation time. Our motivation for formulating the multiscale model of Ca release was to develop a computational framework for relating macroscopic whole-cell behavior to microscopic Ca release processes. This approach is needed for studying the stochastic nature of Ca release dysfunction in cardiac arrhythmias such as Catecholaminergic Polymorphic Ventricular Tachycardia (CPVT) (21). With the stochastic model, one second simulated time required ~ 90 s of run time on Dell PowerEdge™ 2650 Dual Xeon Processor 2U Servers, with dual 2.8 GHz processors. In these simulations, only 1000 out of the total population of 10000 dyads were included, with no appreciable differences in results.

Simulation Methods

A global time step of 0.1 ms is used in the simulations. At each time step, the channel states of the entire population of RyR2 and LCC, and the Ca concentration in each of the dyadic compartments are tracked. The transition rates between LCC and RyR2 states in every dyad are calculated based on the local dyadic Ca concentration. Monte Carlo simulations using these

transition rates determine the state of individual LCCs and RyR2s in the dyad. The Ca fluxes through LCCs and RyR2s are calculated based on the number of open LCCs and RyR2s, respectively, and are used to update local dyadic Ca concentrations. The Ca currents in all individual dyads are added to determine the whole-cell Ca current for a given time step. Reduction in computing time is achieved by assuming quasi-equilibrium condition of Ca_d (11) and by including only a subset of 10,000 dyads in the simulations. Simulation results with 1000 dyads were close to results of the same simulations with a full set of 10,000 dyads. With 1000 dyads, one second simulated time during pacing at 1 Hz, implemented on a 164 processor Linux cluster for high-performance computing, takes about 90 seconds of computing time. All simulation results shown are for 1000 dyads, unless stated otherwise.

Fraction of active dyads and time of Ca release from the dyad

A dyad is assumed to be active when at least 20% of the RyR2s in the dyad are open indicating that a significant amount of Ca release is occurring in the dyad. Start time of Ca release from the dyad is determined as the time at which 20% of RyR2s open.

Ca Spark model

A simulated Ca spark is generated by using Ca efflux from the dyadic space as an input to the buffering and diffusion model of Ca sparks described previously (22), with the exception that we do not take into account optical blurring by confocal microscope.

Impairment of function

In the results section, effects of *complete* impairment of CSQN buffering capacity, luminal sensor function, or inter-dyad coupling are shown, unless stated otherwise. Impaired CSQN buffering capacity was implemented by setting total CSQN to 0.01 mM, thus simulating the role of CSQN as RyR2 regulator only. Impaired luminal Ca sensor regulation was simulated by setting the transition rates between activation and recovery tiers of RyR2 (k_{C1C2}, k_{C2C1}, k_{O1O2} and k_{O2O1}) to zero. To simulate complete impairment of CSQN function (as might occur in a knock-out mouse), both total CSQN concentration and the above transition rates were set to zero.

SUPPLEMENTARY FIGURES

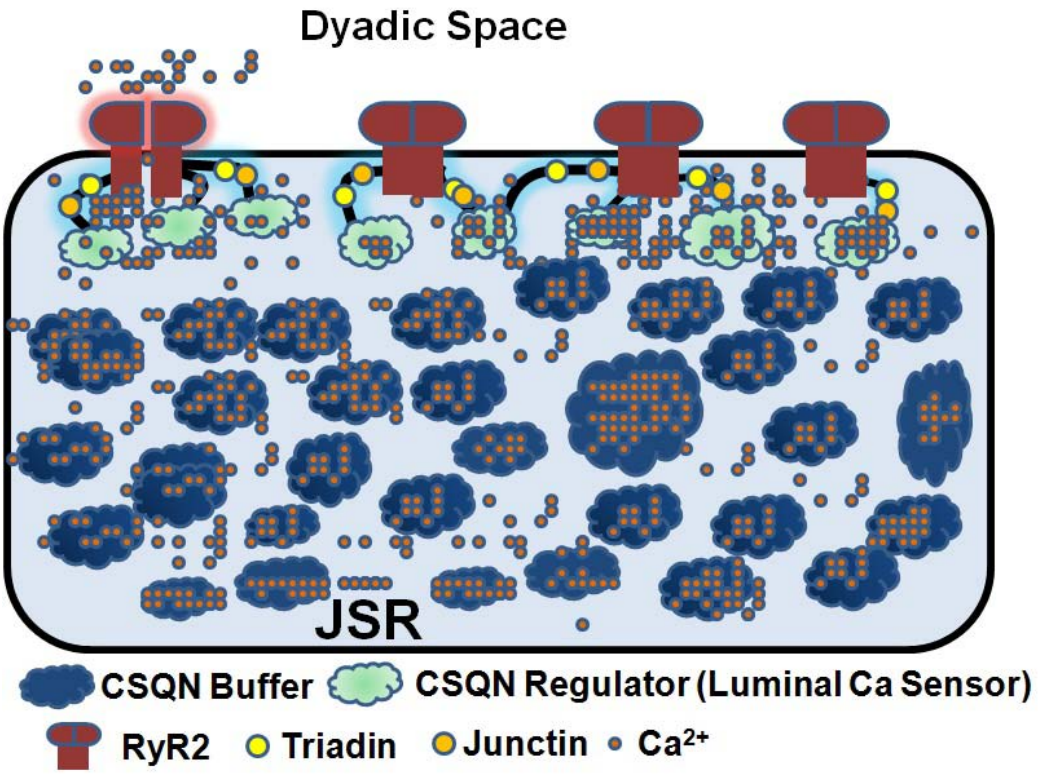

FIGURE S1. Schematic diagram of CSQN function as represented in the model. Each RyR2 senses a proximal portion of CSQN network in its vicinity (CSQN Regulator). The majority of CSQN acts as CSQN Buffer. Junctional Sarcoplasmic Reticulum (JSR) is defined as the domain of CSQN distribution. The Ca buffering properties of CSQN are assumed to be identical throughout the CSQN network. Impaired CSQN buffering capacity was implemented by setting total CSQN to 0.01 mM, thus simulating the role of CSQN as RyR2 regulator only. Impaired luminal Ca sensor regulation was simulated by setting the transition rates between activation and recovery tiers of RyR2 (k_{C1C2}, k_{C2C1}, k_{O1O2} and k_{O2O1}) to zero. To simulate complete impairment of CSQN function (as might occur in a knock-out mouse), both total CSQN concentration and the above transition rates were set to zero.

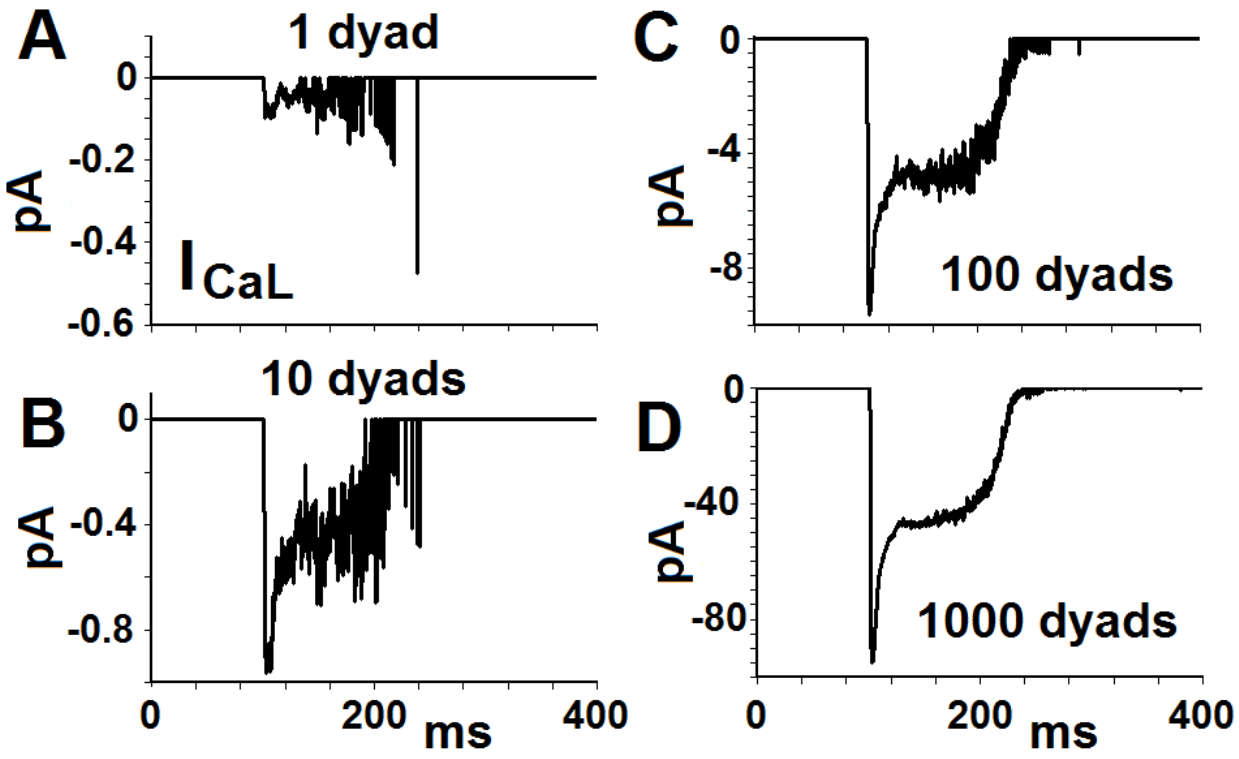

FIGURE S2. L-type Ca current (I_{CaL}) summed over an increasing number of dyads. I_{CaL} through 1 (A), 10 (B), 100 (C) and 1000 (D) dyads. Note that I_{CaL} in dyads approaches I_{CaL}^{cell} as summation is performed over an increasing number of dyads.

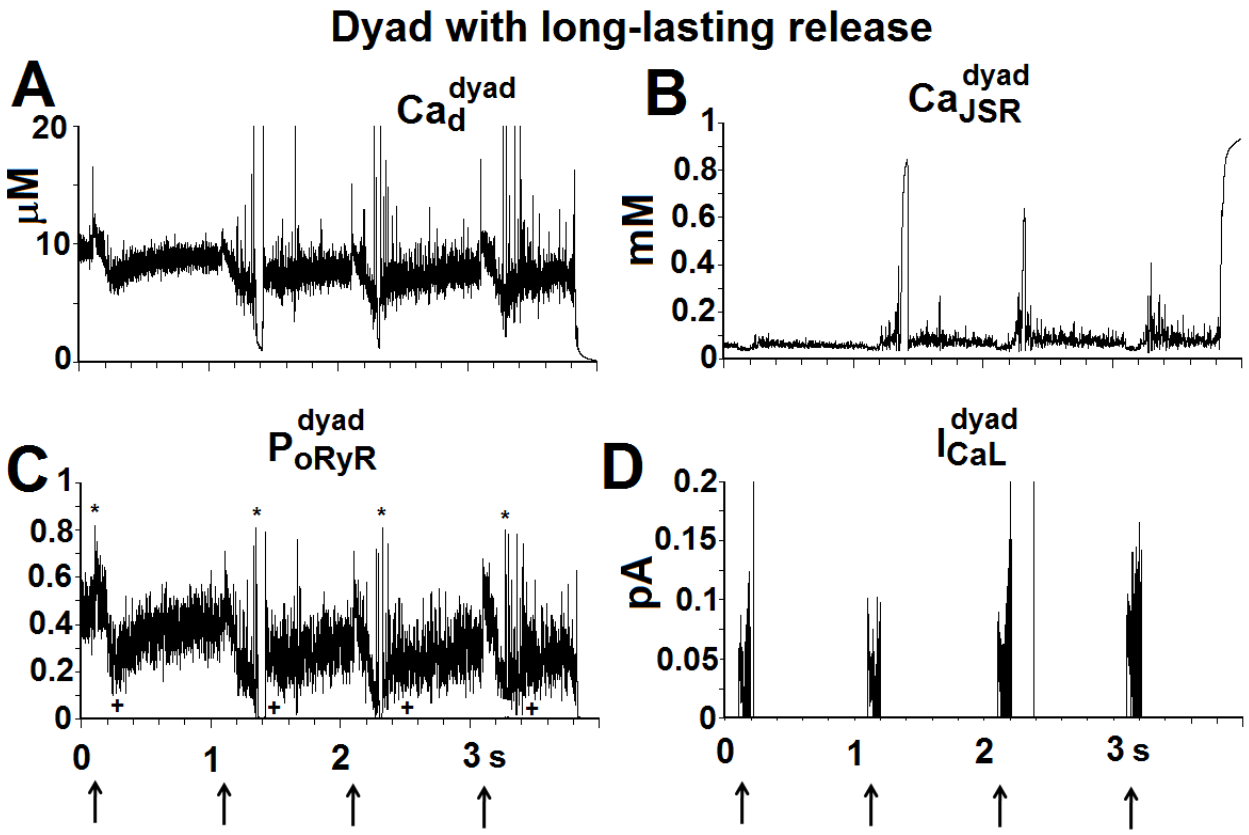

FIGURE S3. Dyadic variables during a long-lasting Ca release event. (A) Dyadic space Ca. (B) JSR Ca. (C) Open fraction of RyR2s. (D) Absolute value of dyadic L-type Ca current. * and + in panel C indicate that the open fraction of RyR2s oscillates approximately between 0.8 and 0.1. Arrows indicate time of pacing stimulus.

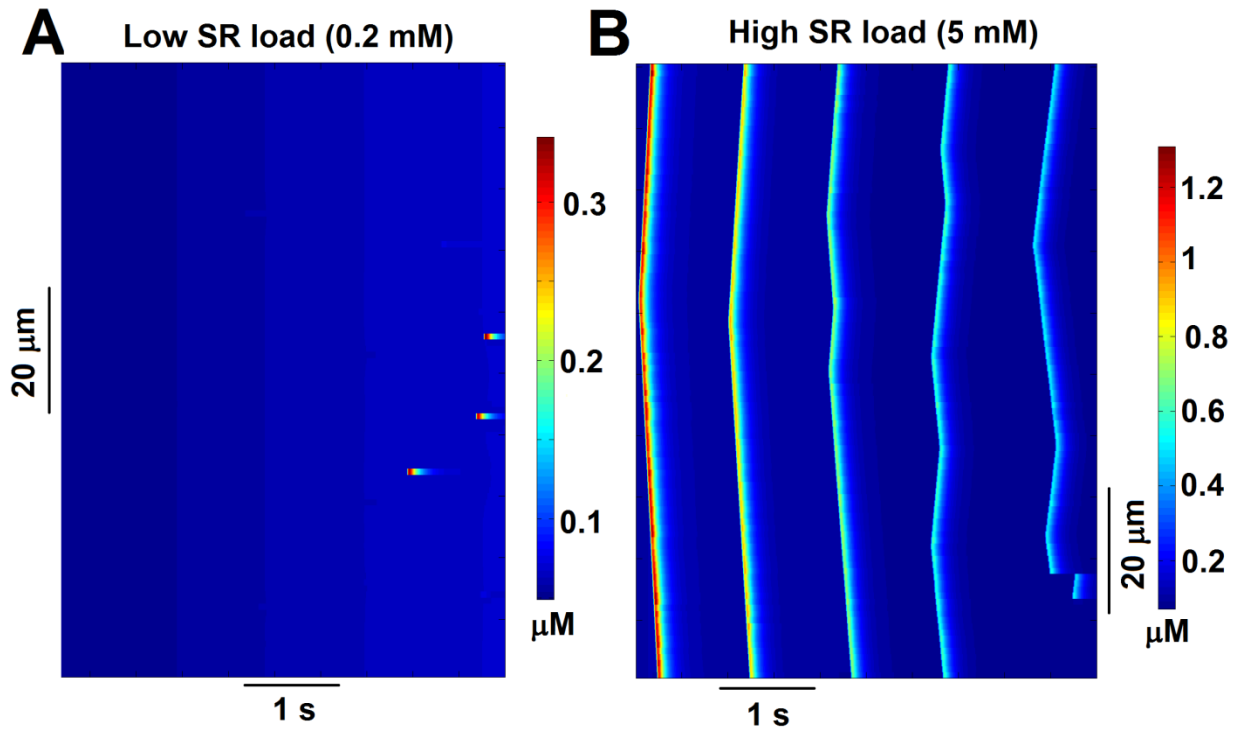

FIGURE S4. Effect of SR Ca load on spontaneous Ca release activity in a quiescent myocyte. (A) Few Ca sparks are seen when the initial SR load was set to a low value of 0.2 mM. (B) Ca waves occur when initial SR load was set to a high value of 5 mM. The duration of simulation is 5 seconds. Ca waves occur during condition of high SR load, similar to experimental observation of Ca waves in Ca overloaded cells.

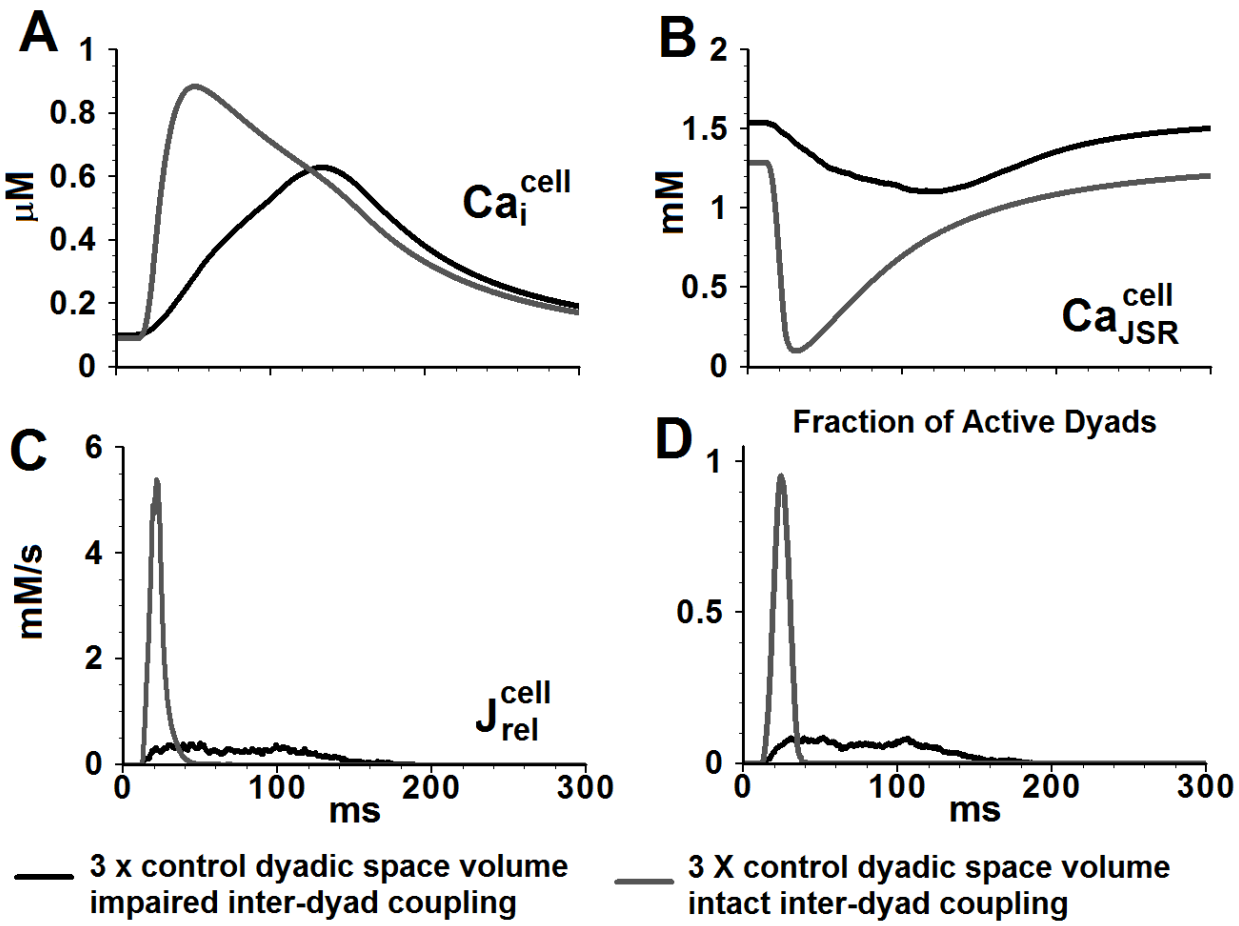

FIGURE S5. Effect of impaired inter-dyad coupling on whole-cell behavior when volume of dyadic space is increased. (A) Myoplasmic Ca transient (Ca_i^{cell}). (B) JSR Ca concentration (Ca_{JSR}^{cell}). (C) Ca release flux (J_{rel}^{cell}). (D) Fraction of active dyads. The myocyte model is paced at 1 Hz.

References

1. Faber, G. M., J. Silva, L. Livshitz, and Y. Rudy. 2007. Kinetic properties of the cardiac L-type Ca^{2+} channel and its role in myocyte electrophysiology: A theoretical investigation. Biophys J 92:1522-1543.

2. Hund, T. J., J. P. Kucera, N. F. Otani, and Y. Rudy. 2001. Ionic charge conservation and long-term steady state in the Luo-Rudy dynamic cell model. Biophys J 81:3324-3331.

3. MacLennan, D. H., and P. T. Wong. 1971. Isolation of a calcium-sequestering protein from sarcoplasmic reticulum. Proc Natl Acad Sci U S A 68:1231-1235.

4. Gyorke, I., N. Hester, L. R. Jones, and S. Gyorke. 2004. The role of calsequestrin, triadin, and junctin in conferring cardiac ryanodine receptor responsiveness to luminal calcium. Biophys J 86:2121-2128.

5. Royer, L., and E. Rios. 2009. Deconstructing calsequestrin. Complex buffering in the calcium store of skeletal muscle. J Physiol 587:3101-3111.

6. Qin, J., G. Valle, A. Nani, H. Chen, J. Ramos-Franco, A. Nori, P. Volpe, and M. Fill. 2009. Ryanodine receptor luminal Ca^{2+} regulation: swapping calsequestrin and channel isoforms. Biophys J 97:1961-1970.

7. Gyorke, I., N. Hester, L. R. Jones, and S. Gyorke. 2004. The role of calsequestrin, triadin, and junctin in conferring cardiac ryanodine receptor responsiveness to luminal calcium. Biophys J 86:2121-2128.

8. Sobie, E. A., K. W. Dilly, J. dos Santos Cruz, W. J. Lederer, and M. S. Jafri. 2002. Termination of cardiac Ca^{2+} sparks: an investigative mathematical model of calcium-induced calcium release. Biophys J 83:59-78.

9. Wu, X., and D. M. Bers. 2006. Sarcoplasmic reticulum and nuclear envelope are one highly interconnected Ca^{2+} store throughout cardiac myocyte. Circ Res 99:283-291.

10. Cheng, H., W. J. Lederer, and M. B. Cannell. 1993. Calcium sparks: elementary events underlying excitation-contraction coupling in heart muscle. Science 262:740-744.

11. Hinch, R. 2004. A mathematical analysis of the generation and termination of calcium sparks. Biophys J 86:1293-1307.

12. Shannon, T. R., F. Wang, J. Puglisi, C. Weber, and D. M. Bers. 2004. A mathematical treatment of integrated Ca dynamics within the ventricular myocyte. Biophys J 87:3351-3371.

13. Jafri, M. S., J. J. Rice, and R. L. Winslow. 1998. Cardiac Ca^{2+} dynamics: the roles of ryanodine receptor adaptation and sarcoplasmic reticulum load. Biophys J 74:1149-1168.

14. Cannell, M. B., and C. Soeller. 1997. Numerical analysis of ryanodine receptor activation by L-type channel activity in the cardiac muscle diad. Biophys J 73:112-122.

15. Sobie, E. A., K. W. Dilly, J. D. Cruz, W. J. Lederer, and M. S. Jafri. 2002. Termination of cardiac Ca^{2+} sparks: An investigative mathematical model of calcium-induced calcium release. Biophys J 83:59-78.

16. Tanskanen, A. J., and R. L. Winslow. 2006. Integrative structurally detailed model of calcium dynamics in the cardiac diad. Multiscale Model Sim 5:1280-1296.

17. Greenstein, J. L., and R. L. Winslow. 2002. An integrative model of the cardiac ventricular myocyte incorporating local control of Ca^{2+} release. Biophys J 83:2918-2945.

18. Greenstein, J. L., R. Hinch, and R. L. Winslow. 2006. Mechanisms of excitation-contraction coupling in an integrative model of the cardiac ventricular myocyte. Biophys J 90:77-91.

19. Restrepo, J. G., and A. Karma. 2009. Spatiotemporal intracellular calcium dynamics during cardiac alternans. Chaos 19:037115.

20. Restrepo, J. G., J. N. Weiss, and A. Karma. 2008. Calsequestrin-mediated mechanism for cellular calcium transient alternans. Biophys J 95:3767-3789.

21. Ylanen, K., T. Poutanen, A. Hiippala, H. Swan, and M. Korppi. 2010. Catecholaminergic polymorphic ventricular tachycardia. Eur J Pediatr 169:535-542.

22. Smith, G. D., J. E. Keizer, M. D. Stern, W. J. Lederer, and H. Cheng. 1998. A simple numerical model of calcium spark formation and detection in cardiac myocytes. Biophys J 75:15-32.